IMD—Software for modeling the optical properties of multilayer films

David L. Windt[a)]

Bell Laboratories, Murray Hill, New Jersey 07974

A computer program called IMD is described. IMD is used for modeling the optical properties (reflectance, transmittance, electric-field intensities, etc.) of multilayer films, i.e., films consisting of any number of layers of any thickness. IMD includes a full graphical user interface and affords modeling with up to eight simultaneous independent variables, as well as parameter estimation (including confidence interval generation) using nonlinear, least-squares curve fitting to user-supplied experimental optical data. The computation methods and user interface are described, and numerous examples are presented that illustrate some of IMD's unique modeling, fitting, and visualization capabilities. © *1998 American Institute of Physics.*
[S0894-1866(98)01604-6]

INTRODUCTION

IMD is a computer program for modeling the optical properties—reflectance, transmittance, absorptance, phase shifts and electric-field intensities—of multilayer films, i.e., films consisting of any number of layers of any thickness. Estimating the optical properties of multilayer films is integral to instrument design and modeling in many fields of science and technology, such as astronomy, lithography, plasma diagnostics, synchrotron instrumentation, etc. Also, fitting the calculated reflectance of a multilayer stack to experimental data is the basis of x-ray reflectance (XRR) analysis of thin films, in which one uses the measured reflectance to determine film thicknesses, densities, and roughnesses and to determine the optical constant from reflectance versus incidence-angle data, a technique utilized in many spectral regions.[1] IMD was designed, therefore, as a completely general modeling and parameter-estimation tool, intended to be used for these and other applications, in order to meet the needs of a broad range of researchers. Furthermore, IMD's flexibility enables many new and unique types of computations. IMD is available free via the Internet.[2]

In IMD, a layer can be composed of any material for which the optical constants are known or can be estimated. Any number of such layers can be designated and optionally grouped together to define periodic multilayers; "groups of groups" of layers can be defined, in fact, with no limit on nesting depth. The IMD distribution includes an optical-constant database for over 150 materials, spanning the x-ray to the far-infrared region of the spectrum. User-defined optical constants can be used as well, and in the 30 eV–30 keV region in particular, optical constants can be generated by the user for arbitrary compounds using the CXRO atomic scattering factors.[3] Imperfections at an interface, i.e., roughness and/or diffuseness, can be easily included; the effect of such imperfections, namely, to reduce the specular reflectance at the interface, becomes especially important at shorter wavelengths (i.e., below ~ 30 nm), where the length scale of these imperfections is comparable to the wavelength of light.

The optical functions (reflectance, transmittance, etc.) can be computed not just versus wavelength and/or incidence angle, but also as a function of any of the parameters that describe the multilayer stack (e.g., layer thicknesses, roughnesses, etc.) or the incident beam (polarization, angular/spectral resolution). An interactive visualization tool, IMDXPLOT, is used to display the results of such multiple-variable computations; with this visualization tool one can vary a given parameter and see the resulting effect on the optical functions (in one or two dimensions) in real time. This latter feature is especially helpful in discerning the relative sensitivities of the optical functions to the parameters that describe the multilayer structure.

Parameter estimation is afforded by fitting an optical function to user-supplied experimental data: nonlinear, least-squares curve fitting based on the χ^2 test of fit is utilized. The precision of the best-fit parameters can be estimated as well by computing multidimensional confidence intervals. The ability to simultaneously vary multiple parameters "manually," as mentioned above, prior to performing least-squares fitting, is particularly useful in selecting initial parameter values; indeed, choosing initial fit parameter values that are reasonably close to the best-fit values is generally the most difficult aspect of multiparameter nonlinear fitting.

IMD is written in the IDL language,[4] and makes extensive use of IDL's built-in "widgets" to provide a full graphical user interface. As such, IMD can be run on most (currently) popular platforms, including MacOS, MS Windows, and most flavors of Unix.

In the following, we will describe first the physics and algorithms used for modeling and parameter estimation,

---

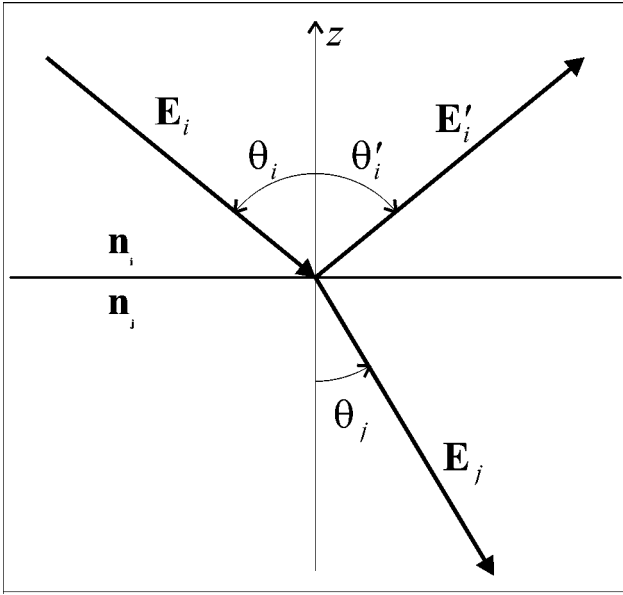[a)]E-mail: windt@bell-labs.com; www.bell-labs.com/user/windt

Figure 1. Diagram of a plane wave incident at the interface between two optically dissimilar materials.

Figure 2. Sketch of the interface profile function $p(z)$, which describes a rough or diffuse interface.

followed by a description of the IMD user interface. Finally, we present several illustrative examples, demonstrating IMD's unique modeling and fitting capabilities.

I. COMPUTATION METHODS

A. Optical functions

Computations of the optical functions of a multilayer film in IMD are based on application of the Fresnel equations, modified to account for interface imperfections, which describe the reflection and transmission of an electromagnetic plane wave incident at an interface between two optically dissimilar materials.

1. Reflection and transmission at an ideal interface : We consider first the behavior of a plane electromagnetic wave at an idealized interface, i.e., the abrupt interface between two semi-infinite media, as shown in Fig. 1. The complex index of refraction $\mathbf{n} = n + ik$ (where n is the refractive index and k is the extinction coefficient) is given in the two regions as $\mathbf{n}_i$ and $\mathbf{n}_j$. The incident wave vector, with electric-field amplitude $\mathbf{E}_i$, makes an angle θ_i with respect to the interface normal (the z axis). The amplitude of the reflected and transmitted electric fields, $\mathbf{E}_i'$ and $\mathbf{E}_j$, respectively, are given by the well-known Fresnel equations:[5]

$$\frac{|\mathbf{E}_i'|}{|\mathbf{E}_i|} = \frac{\mathbf{n}_i \cos\theta_i - \mathbf{n}_j \cos\theta_j}{\mathbf{n}_i \cos\theta_i + \mathbf{n}_j \cos\theta_j} \equiv r_{ij}^s \tag{1a}$$

and

$$\frac{|\mathbf{E}_j|}{|\mathbf{E}_i|} = \frac{2\mathbf{n}_i \cos\theta_i}{\mathbf{n}_i \cos\theta_i + \mathbf{n}_j \cos\theta_j} \equiv t_{ij}^s, \tag{1b}$$

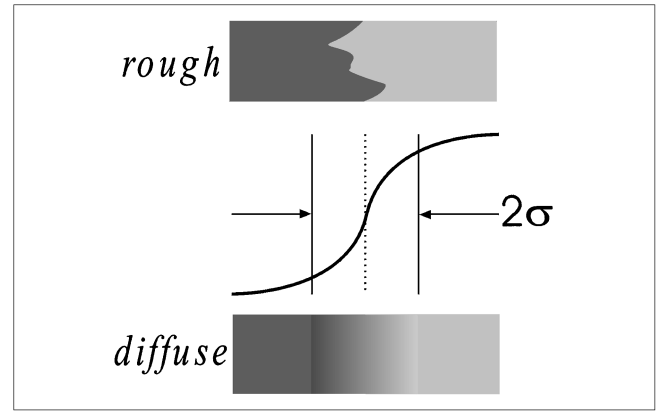for s polarization (i.e., $\mathbf{E}$ perpendicular to the plane of incidence); and

$$\frac{|\mathbf{E}_i'|}{|\mathbf{E}_i|} = \frac{\mathbf{n}_i \cos\theta_j - \mathbf{n}_j \cos\theta_i}{\mathbf{n}_i \cos\theta_j + \mathbf{n}_j \cos\theta_i} \equiv r_{ij}^p \tag{1c}$$

and

$$\frac{|\mathbf{E}_j|}{|\mathbf{E}_i|} = \frac{2\mathbf{n}_i \cos\theta_i}{\mathbf{n}_i \cos\theta_j + \mathbf{n}_j \cos\theta_i} \equiv t_{ij}^p \tag{1d}$$

for p polarization (i.e., $\mathbf{E}$ parallel to the plane of incidence), where θ_j is the angle of refraction, determined from Snell's law: $\mathbf{n}_i \sin\theta_i = \mathbf{n}_j \sin\theta_j$. In Eq. (1) we have introduced the Fresnel reflection and transmission coefficients, r_{ij} and t_{ij}, respectively.[6]

2. Interface imperfections : In order to account for the loss in specular reflectance due to interface imperfections (i.e., interfacial roughness and/or diffuseness), we now consider the case where the change in index across the interface is not abrupt, but can be described instead by an interface profile function $p(z)$ (see Fig. 2). That is, following the formalism developed by Stearns,[7] we define $p(z)$ as the normalized, average value along the z direction of the dielectric function, $\varepsilon(\mathbf{x})$ (with $\mathbf{n} = \sqrt{\varepsilon}$):

$$p(z) = \frac{\int\int \varepsilon(\mathbf{x}) dx\, dy}{(\varepsilon_i - \varepsilon_j)\int\int dx\, dy}, \tag{2}$$

where

$$\varepsilon(\mathbf{x}) = \begin{cases} \varepsilon_i, & z \to +\infty, \\ \varepsilon_j, & z \to -\infty. \end{cases} \tag{3}$$

Stearns has shown that in the case of nonabrupt interfaces, the resultant loss in specular reflectance can be approximated by multiplying the Fresnel reflection coefficients [Eqs. (1a) and (1c)] by the function $\widetilde{w}(s)$, the Fourier transform of $w(z) = dp/dz$. That is, the modified Fresnel reflection coefficients are given by

$$r_{ij}' = r_{ij}\widetilde{w}(s_i), \tag{4}$$

Table I. Interface profile functions, $p(z)$, and the associated Fresnel reflection coefficient modification factors $\widetilde{w}(s)$ (from Ref. 7) available for use in IMD.

	$p(z)$	$\widetilde{w}(s)$
Error function	$\dfrac{1}{\sqrt{\pi}}\displaystyle\int_{-\infty}^{z} e^{-t^2/2\sigma^2}\,dt$	$e^{-s^2\sigma^2/2}$
Exponential	$\begin{cases}\frac{1}{2}e^{\sqrt{2}z/\sigma}, & z\le 0 \\[4pt] 1-\frac{1}{2}e^{\sqrt{2}z/\sigma}, & z>0\end{cases}$	$\dfrac{1}{1+s^2\sigma^2/2}$
Linear	$\begin{cases}0, & z<-\sqrt{3}\sigma \\[4pt] \frac{1}{2}+\frac{z}{2\sqrt{3}\sigma}, & |z|\le\sqrt{3}\sigma \\[4pt] 1, & z>-\sqrt{3}\sigma\end{cases}$	$\dfrac{\sin(\sqrt{3}\sigma s)}{\sqrt{3}\sigma s}$
Sinusoidal	$\begin{cases}0, & z<-a\sigma \\[4pt] \frac{1}{2}+\frac{1}{2}\sin\left(\frac{\pi z}{2a\sigma}\right), & |z|\le a\sigma \\[4pt] 1, & z>a\sigma\end{cases}$ $a=\pi/\sqrt{\pi^2-8}$	$\dfrac{\pi}{4}\left(\dfrac{\sin(a\sigma s-\pi/2)}{a\sigma s-\pi/2}+\dfrac{\sin(a\sigma s+\pi/2)}{a\sigma s+\pi/2}\right)$

where $s_i = 4\pi\cos\theta_i/\lambda$, and λ is the wavelength of light. Note that the loss in specular reflectance depends only on the *average* variation (over x and y) in index across the interface. Consequently, the reflectance can be reduced equally well by either a rough interface, in which the transition between the two materials is abrupt at any point (x,y), or a diffuse interface, in which the index varies smoothly along the z direction (or by an interface that can be described as some combination of the two cases).

Stearns presents four particularly useful interface profiles, all of which are available for use in IMD; these interface profile functions and the associated $\widetilde{w}(s)$ functions are listed in Table I. Also available in IMD are modified $\widetilde{w}(s)$ functions, where s_i has been replaced with $s_{ij} = 4\pi\sqrt{\cos\theta_i\cos\theta_j}/\lambda$, in accord with the formalism developed by Névot and Croce[8] to properly account for the effect of roughness on the specular reflectance below the critical angle of total external reflection in the x-ray region.

The width of each interface profile function presented in Table I is characterized by the parameter σ (see Fig. 2), which is a measure of either a root-mean-square (rms) interfacial roughness in the case of a purely rough interface, an interface width in the case of a purely a diffuse interface, or some combination of the two properties in the case of an interface that is both rough and diffuse; it is the parameter σ (along with the choice of interface profile function) that is specified in IMD to account for the effects of interface imperfections using the modified Fresnel coefficient approach just described.

3. Optical functions of a multilayer stack : We now consider a plane wave incident on a multilayer stack, that is, a series of N layers (and $N+1$ interfaces), where the ith layer has thickness d_i, interfacial roughness/diffuseness σ_i, and optical constants $\mathbf{n}_i$, as shown in Fig. 3. The region above the multilayer stack—the ambient—has optical constants $\mathbf{n}_a$, and the region below the film—the substrate—has optical constants $\mathbf{n}_s$. (Note that the case of a free-standing film refers to the condition $\mathbf{n}_s=\mathbf{n}_a$.) Under these circumstances, the net reflection (r_i) and transmission (t_i) coefficients of the ith layer are given by[9]

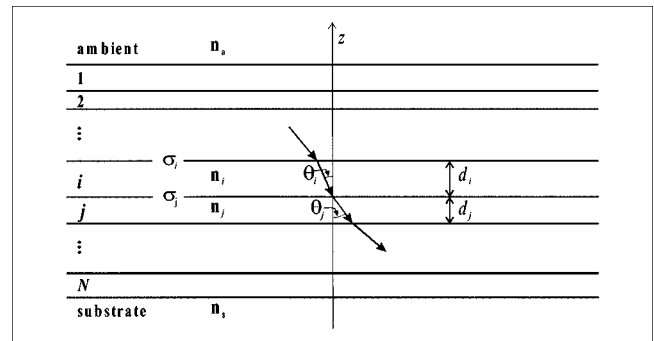$$r_i = \frac{r_{ij}+r_j e^{2i\beta_i}}{1+r_{ij}r_j e^{2i\beta_i}}, \qquad (5a)$$

Figure 3. Diagram of a multilayer stack containing N layers, where the optical constants, thickness, propagation angle, and interface roughness/ diffuseness parameter of the ith layer are $\mathbf{n}_i$, d_i, θ_i, and σ_i, respectively. The ambient (i.e., the region above the film) has optical constants $\mathbf{n}_a$, and the substrate has optical constants $\mathbf{n}_s$.

and

$$t_i = \frac{t_{ij}t_j e^{2i\beta_i}}{1+r_{ij}r_j e^{2i\beta_i}}, \tag{5b}$$

where $\beta_i = 2\pi d_i \mathbf{n}_i \cos\theta_i/\lambda$; the reflection coefficients r_{ij} are computed from Eq. (4), the transmission coefficients t_{ij} from Eqs. (1b) and (1d), and r_j and t_j are the net reflection and transmission coefficients of the jth interface. Thus, the procedure to compute the net reflection (r) and transmission (t) coefficients for the multilayer stack is to apply Eq. (5) recursively, starting at the bottom-most layer, i.e., $i = N$, $j = s$. (The coefficients r and t for s and p polarization are computed separately using the appropriate Fresnel coefficients.) The reflectance R and transmittance T, which measure the energy reflected from or transmitted through the film, respectively, are then given by

$$R = |r|^2 \tag{6a}$$

and

$$T = \mathrm{Re}\left\{ \frac{\mathbf{n}_s \cos\theta_s}{\mathbf{n}_a \cos\theta_a} \right\} |t|^2 \tag{6b}$$

(again, separately computing the values for s and p polarization, i.e., R^s, R^p, T^s, and T^p). The absorptance, A, which measures the amount of energy absorbed by the film, is approximated by

$$A = 1 - R - T. \tag{6c}$$

[Note that Eq. (6c) is inaccurate when light is removed from the specular direction, i.e., and scattered into non-specular directions, due to interfacial or surface roughness.] Finally, the phases of the reflected and transmitted waves are given by

$$\phi_r = \tan^{-1}(\mathrm{Im}\{r\}/\mathrm{Re}\{r\}) \tag{7a}$$

and

$$\phi_t = \tan^{-1}(\mathrm{Im}\{t\}/\mathrm{Re}\{t\}). \tag{7b}$$

4. Electric-field intensity in a multilayer stack : In order to compute, in addition to the optical functions, the electric-field intensity as a function of depth in a multilayer stack, a slightly different formalism from that described in Sec. I A 3 must be used. (The previous, more efficient, formalism is used in IMD when electric-field intensities are not required.) Let us consider the interface between the ith and the jth layers in a multilayer stack, where we now have both positive-going and negative-going electromagnetic plane waves in both layers. Solving Maxwell's equations in this case, we can show that the positive-going and negative-going field amplitudes at a distance z_i above the interface are given by

$$E_i^+(z_i) = \frac{1}{t_{ij}}e^{-i\beta_i(z_i)}E_j^+(0) + \frac{r_{ij}}{t_{ij}}e^{-i\beta_i(z_i)}E_j^-(0) \tag{8a}$$

and

$$E_i^-(z_i) = \frac{r_{ij}}{t_{ij}}e^{i\beta_i(z_i)}E_j^+(0) + \frac{1}{t_{ij}}e^{i\beta_i(z_i)}E_j^-(0), \tag{8b}$$

respectively, where $\beta_i(z_i) = 2\pi z_i \mathbf{n}_i \cos\theta_i/\lambda$, and $E_j^+(0)$ and $E_j^-(0)$ are the field amplitudes at the top of the jth layer. Again, a recursive approach can be used to compute the field amplitudes throughout the stack, starting at the bottom-most layer ($i = N$, $j = s$) with the field amplitudes in the substrate given as $E_s^+(0) = 1$ and $E_s^-(0) = 0$. The net reflection and transmission coefficients of the film can then be computed from the field amplitudes in the ambient:

$$r = \frac{E_a^-(0)}{E_a^+(0)}, \tag{9a}$$

and

$$t = \frac{1}{E_a^+(0)}. \tag{9b}$$

Once the transmission coefficient is computed from Eq. (9b), the field amplitudes versus depth are then rescaled using

$$E^\pm(z) \rightarrow tE^\pm(z) \tag{10}$$

(i.e., by taking the incident electric field to have unit amplitude) and the field intensities for s and p polarization are computed from

$$I(z) = |E^+(z) + E^-(z)|^2. \tag{11}$$

5. Polarization : In the case of an incident beam that consists of a mixture of s and p polarization, it is often necessary to compute the "average" values of the optical functions R, T, and A, and the electric-field intensity I, i.e., the values of these quantities for "average" polarization. We thus define the incident polarization factor f as

$$f = \frac{I^s - I^p}{I^s + I^p}, \tag{12}$$

where I^s and I^p are the incident intensities for s and p polarization (e.g., unpolarized radiation corresponds to $f = 0$). Furthermore, we define the polarization-analyzer sensitivity, q, as the sensitivity to s polarization divided by the sensitivity to p polarization; specifying a value of q other than 1.0 could be used to simulate, for example, the reflectance one would measure using a detector that (for whatever reason) was more or less sensitive to s polarization than to p polarization. It can be shown that the average reflectance is then given by

$$R^a = \frac{R^s q(1+f) + R^p(1-f)}{f(q-1) + (q+1)}, \tag{13}$$

with equivalent expressions for T^a, A^a and I^a.

6. Instrumental resolution : In general, the experimental determination of an optical function such as R, T, or A is made with instrumentation that is limited in angular and/or
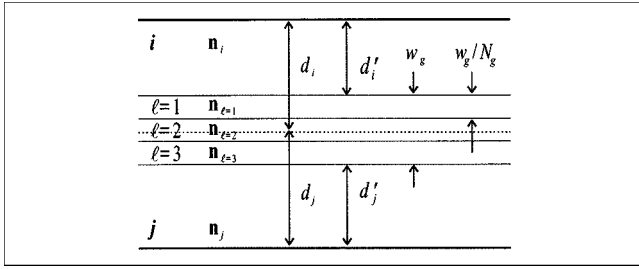
Figure 4. Diagram of a graded interface of width w_g, consisting of N_g = 3 layers. In this case, the distribution parameter X_g is slightly less than 0.5.

spectral resolution. As such, it is desirable to estimate resolution-limited values of the calculated optical functions. This is achieved in IMD by convolving the calculated optical functions with a Gaussian of width $\delta\theta$, in the case of finite angular resolution, or with a Gaussian of width $\delta\lambda$, in the case of finite spectral resolution, using the convolution algorithm built into IDL.

7. Graded interfaces : In addition to the option of using the modified Fresnel coefficients to account for interfacial roughness and diffuseness, as described in Sec. I A2, in IMD it is also possible to model the effects of a diffuse interface on the optical functions and electric-field intensities by specifying a ''graded'' interface. That is, an abrupt interface can be replaced by one or more layers whose optical constants vary gradually between the values for the pure materials on either side of the interface.

In IMD, a graded interface is described by three parameters, as shown in Fig. 4: the interface width, w_g, the number of layers comprising the graded interface, N_g, and the distribution factor, X_g, which determines where the graded interface region resides relative to the original abrupt interface (as will be described below).

The optical constants in each of the N_g layers of a graded interface are computed as follows. Consider the graded interface between the ith and jth layers in a multilayer stack. The thickness of each of the N_g graded interface layers is equal to w_g/N_g. The optical constants in the ℓth graded interface layer are thus given by

$$n_\ell = \frac{(N_g+1-\ell)n_i+\ell n_j}{(N_g+1)} \qquad (14a)$$

and

$$k_\ell = \frac{(N_g+1-\ell)k_i+\ell k_j}{(N_g+1)}, \qquad (14b)$$

with $\ell = 1, \ldots, N_g$. The resulting layer thicknesses, d_i' and d_j', of the pure materials in the ith and jth layers, respectively, after including the graded interface layers, are given by

$$d_i' = d_i - w_g(1-X_g) \qquad (15a)$$

and

$$d_j' = d_j - w_g X_g, \qquad (15b)$$

with $0 < X_g < 1$. (Note that the total thickness of the two layers—including all the graded interface layers—is constant, i.e., $d_i' + d_j' + w_g = d_i + d_j$.) As an example, a distribution factor of 50% ($X_g = 0.5$) would result in equal reductions of the ith and jth layer thicknesses.

B. Parameter estimation

As will be described in Sec. II B, it is possible in IMD to designate simultaneously up to eight independent variables when computing optical functions and electric-field intensities. When attempting to model experimental optical data, however, it is often desirable to estimate parameter values automatically, using nonlinear, least-squares curve fitting. To this end, parameter estimation based on the χ^2 test of fit can be used in IMD to determine any number of parameters that describe the multilayer stack (or the incident-beam polarization and/or instrumental resolution), as will now be described.

1. Fitting algorithm : We consider a one-dimensional optical function $Y(X)$ for a multilayer stack, where Y may be any one of R^a, T^a, or A^a, and X is some independent variable (e.g., λ, θ, etc.). The values for $Y(X)$ depend on the values of all the parameters that describe the multilayer stack (optical constants, layer thicknesses, etc.) and the incident beam (polarization, instrumental resolution, etc.). The problem we wish to solve is the following: determine the values for some fixed number p of these adjustable parameters, such that the calculated optical function $Y(X)$ most closely fits a particular set of experimentally determined optical data, $Y_m \pm \delta Y_m$, measured as a function of the independent variable X_m, where X_m takes on $i = 1, \ldots, N_m$ discrete values.

To solve this problem, IMD makes use of the so-called Marquardt gradient-expansion algorithm,[10] based on the χ^2 test,[11] in which we minimize the value of the statistic S, defined as

$$S \equiv \sum_{i=1}^{N_m} \frac{(Y[i] - Y_m[i])^2}{w[i]^2}, \qquad (16)$$

where $w[i]$ are the weighting factors for each point. IMD uses the CURVEFIT procedure,[11] an adaptation of the Marquardt algorithm included in the IDL library. The user designates adjustable parameters, and initial values for each. (In IMD, a constraint on the range of acceptable parameter values can be specified as well.) Iterations are then performed until the change in S is less than a specified amount or until a maximum number of iterations has been performed. The user can choose to use for $w[i]$ either (a) ''instrumental weighting,'' using the experimental uncertainties, $w[i] = \delta Y_m[i]$, (b) ''statistical weighting,'' with $w[i] = \sqrt{Y_m[i]}$, or (c) ''uniform weighting,'' with $w[i] = 1$. Additionally, logarithmic fitting can be used, in which the numerator in Eq. (16) is replaced by $(\ln Y[i] - \ln Y_m[i])^2$.

2. Confidence interval computation : In addition to a point-estimate determination of the ''best-fit'' parameter values, using the fitting technique just described, for example, it is generally necessary to estimate also the *range* of acceptable parameter values that are consistent with the experimental data. To this end, in IMD it is possible to compute multidimensional confidence intervals associated with the best-fit values of the adjustable parameters using the formalism described in Refs. 12 and 13.

It can be shown that, when using the χ^2 test of fit, the minimum value of the S statistic, $S_{\min}$, associated with the best-fit parameter values, is distributed as the χ^2 probability function with $N_m - p$ degrees of freedom:

$$S_{\min} = \chi^2_{N_m - p}(\alpha), \qquad (17)$$

where α is the significance of fit. That is, if we find, for example, that $S_{\min} = \chi^2_{N_m - p}(0.68)$, then we can conclude that there is a 68% probability that the model (using the p best-fit parameter values) correctly describes the data.

The confidence region, with significance α', is then defined as the p-dimensional region of parameter space for which the value of S is less than or equal to some value S_L, where

$$S_L = S_{\min} + \Delta S(\alpha'), \qquad (18)$$

with $\Delta S(\alpha')$ equal to the value of the χ^2 probability function with p degrees of freedom and significance α'; the confidence region so defined would enclose the true values of the p parameters in $1 - \alpha'$ of all experiments.

In IMD, a multidimensional confidence region can be determined for up to eight adjustable (i.e., fit) parameters simultaneously. In this case a grid-search algorithm is utilized, wherein the user specifies the extent and resolution of the grid along each parameter axis. At each point in the grid, the value of the statistic S is computed using one of two methods, depending on the dimensionality of the confidence region being determined. That is, suppose the best-fit parameters were determined by varying p adjustable parameters, as described above, and of these p parameters, we are interested in the confidence region associated with some subset of parameters, q, where $q \leq p$. In the case that $q = p$, the value of S at each point on the grid is determined directly from Eq. (16). On the other hand, in the case where $q < p$, the value of S at each point on the grid is determined in IMD using the minimization algorithm described in Sec. I B1, but with only $(p - q)$ adjustable parameters, i.e., q of the parameters are now fixed. In this case, we note that the correct value of $\Delta S(\alpha')$ to be used in Eq. (18) is equal to the value of the χ^2 probability function with q (not p) degrees of freedom and significance α'. As an example of a situation for which $q < p$, consider the case of making a determination of thin-film optical constants from reflectance versus incidence-angle data, where three adjustable parameters have been used, say—the optical constants n and k, and the film thickness, d—but of these three parameters, we are interested only in the uncertainty on the derived values of n and k, and so we must compute the as-
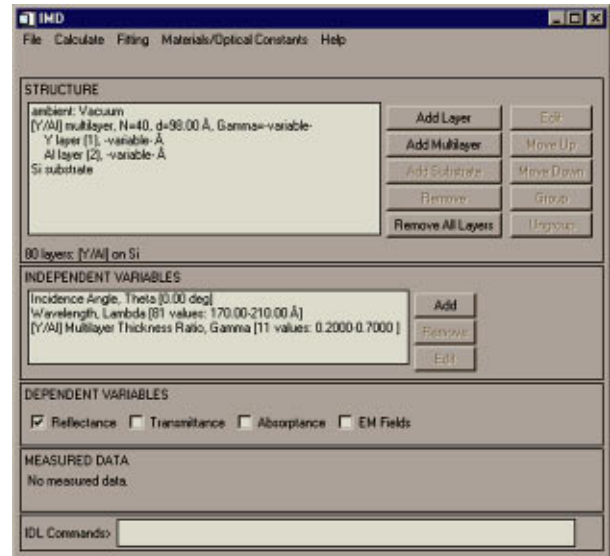

Figure 5. The main IMD widget, configured to compute the normal incidence reflectance of a Y/Al multilayer as a function of wavelength and layer thickness parameter Γ. (The results of this particular computation are presented in Sec. III B.)

sociated two-dimensional confidence region in n-k space. A specific example of a confidence-interval computation that illustrates the concepts described here will be presented in Sec. III D.
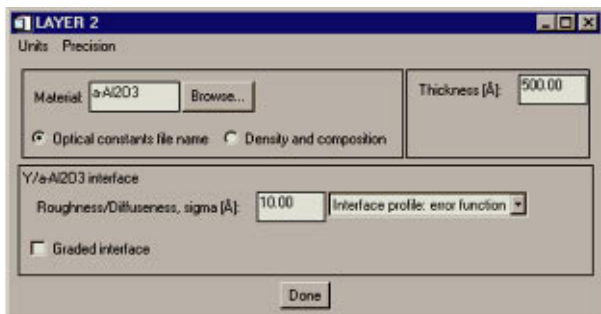
II. USER INTERFACE

We now describe the IMD graphical user interface (GUI). This interface, which is created from the widgets tool kit built into IDL, is used to specify all parameters and variables and to visualize the results of all calculations.

Shown in Fig. 5 is the main IMD widget as it might look after a periodic multilayer and associated independent and dependent variables have been specified. In addition to the menu bar at the top of the widget, there are three regions of this widget of particular interest to us now: the STRUCTURE region, and the INDEPENDENT and DEPENDENT VARIABLES regions.
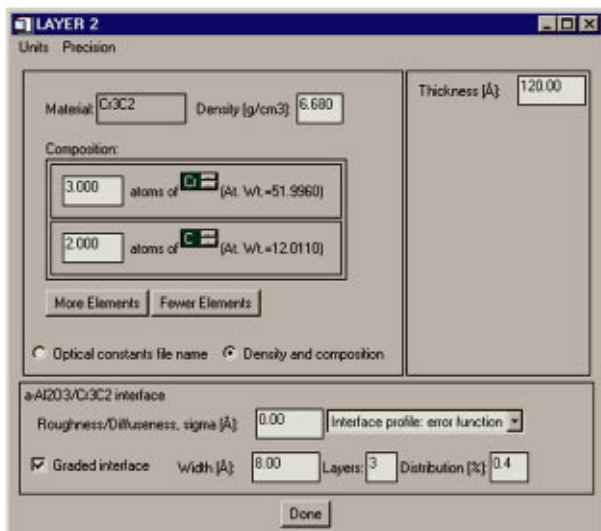
A. Structure specification

The first step in performing a calculation in IMD is defining the ''structure,'' i.e., the parameters that define the ambient material, the multilayer stack, and (optionally) a substrate. A number of parameters can be assigned to each structure element, i.e., layer thicknesses, interface roughness/diffuseness parameters, etc. But common to all structure elements is the material designation, which determines which optical constants are used for the calculation, and that is described in Sec. II A1.

1. Material designation : Each structure element—the ambient, the substrate, and each multilayer-stack layer element—is composed of some material. There are two different methods available to the user to designate materials in IMD: in the first method, the designated material name refers to an optical-constants file contained in the IMD

Figure 6. A typical IMD layer widget, with material designation (a) by reference to an optical constants file, and (b) by specification of material composition and density.

optical-constant database; in the second method, which is applicable only in the x-ray region for energies between 30 eV and 30 keV, the material is specified by its composition and density, and the optical constants are computed directly from the atomic scattering factors.

The IMD optical-constants database is a directory of ASCII files, in which each optical-constants file contains three columns of optical data (λ, n, and k) associated with a single material. To designate a material by reference to an optical-constants file, the user need only specify a valid file name contained in the optical constants directory. For example, shown in Fig. 6(a) is a typical IMD layer widget where the material has been designated as amorphous Al_2O_3, i.e., corresponding to a file called a-Al2O3.nk.

The IMD optical-constants database contains data for over 150 materials, compiled from a variety of published sources, with wavelength coverage extending from the x-ray to the far-infrared region of the spectrum. In order to use additional optical constants, a user need only create an ASCII file containing the optical constants for the desired material in accord with a simple format specified in the IMD documentation. For many materials, the user can

choose from among several data sets already available in the database. The contents of any of the files contained in the database can be displayed graphically using an interactive plot widget, available through a pull-down menu option from the main IMD widget.

The basis for the second method of material designation—by composition and density—is that in the x-ray region, the complex index of refraction for a compound of density ρ is related to the atomic scattering factors f_1 and f_2 by[3]

$$\mathbf{n} \cong 1 - \frac{e^2 N_a}{2\pi m_e c^2}\lambda^2 \rho \frac{\Sigma_j x_j (f_{1,j} + i f_{2,j})}{\Sigma_j x_j A_j}, \qquad (19)$$

where the sums range over each of the chemical elements that compose the compound, the x_j are the relative concentrations of each element, and the A_j are the associated atomic densities; e, m_e, c, and N_a are the electron charge, the electron mass, the speed of light, and Avogadro's number, respectively. To utilize this method of material designation, the user must specify the atomic composition (i.e., the x_j) and the density of the material, as illustrated in Fig. 6(b), for example, showing the layer widget for a layer composed of Cr_3C_2 having a density of 6.68 g/cm^3.

2. Layer and group parameters : To create an IMD structure, the user adds layers, periodic multilayers,[14] and optionally a substrate if desired. Accomplishing these tasks is simply a matter of pushing the appropriate buttons on the main IMD widget (i.e., on the right side of the STRUCTURE area of the widget shown in Fig. 5). Layers and periodic multilayers can be subsequently grouped together to form higher-level periodic multilayers (with no limit on nesting depth), and can be moved up or down in the stack, again by pushing the appropriate buttons. The structure components are listed on the main IMD widget (on the left side), and by double clicking on a structure element, the associated ambient, layer, multilayer, or substrate widget is created, allowing the user to specify the adjustable parameters (e.g., materials, layer thicknesses, interface parameters, multilayer repeat periods, etc.), as well as the preferred units (i.e., Å, nm, μm, etc.), and the displayed precision of parameter values. Thus, rather complicated structures can be defined or changed easily, and in a matter of minutes.

B. Variable designation

For all calculations, at least one wavelength (or energy) and incidence angle must be specified; multiple wavelengths and/or angles can be specified as well, if desired. (In the case of electric-field-intensity calculations, a third independent variable—depth, i.e., the position in the structure, measured from the top of the first layer—must also be defined.) In addition to these variables, any of the parameters that describe the multilayer stack (i.e., layer thicknesses, interface σ values, graded-interface parameters, multilayer parameters, etc.) or the incident beam (i.e., polarization parameters, f and q, and angular and spectral resolution) can be designated as independent variables; up to eight independent variables can be designated simultaneously, and

the dimensionality of the resulting optical functions will be equal to the number of independent variables specified.

For every independent variable so designated, the user must define the extent and resolution of the grid of points over which the optical functions are to be computed. The resolution of the grid can be designated either by specifying the size of the increment between points, or by the total number of parameter values that compose the independent variable; logarithmically spaced grids can also be designated. The user can again specify the preferred precision and units, and in the case of wavelengths (or energies) the instrumental resolution and polarization parameters; the angular instrumental resolution is likewise specified using the incidence-angle independent-variable widget.

Once the structure and independent variables are defined, any or all of the optical functions R, T, and A, and the electric-field intensity, I, can be computed by selecting these functions in the DEPENDENT VARIABLES area of the main IMD widget (see Fig. 5). By then choosing the appropriate menu option, the computation is performed and the results displayed using another GUI tool, IMDXPLOT. Specific examples illustrating the functionality of IMDXPLOT will be presented in Sec. III.
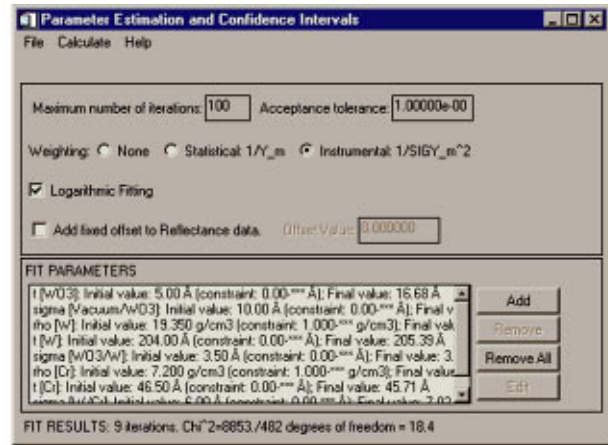
C. Fit-parameter designation

As was discussed in Sec. I B, parameter estimation using nonlinear, least-squares fitting can be performed utilizing user-supplied experimental data. The experimental data is read by accessing a menu option from the main IMD widget, and the parameter-estimation and confidence-interval widget, shown in Fig. 7(a), allows the user to add and remove adjustable (fit) parameters and to specify the parameters that control how the fitting is performed (i.e., number of iterations, weighting, etc.). Shown in Fig. 7(b) is a typical fit-parameter widget, wherein the user specifies the initial parameter value (and optionally constraints on the fit parameter), as well as the parameters associated with confidence-interval computations, as described in Sec. I B2.
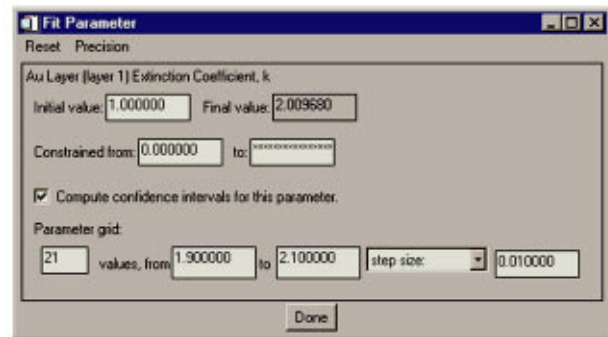
III. EXAMPLES

A. Multidimensional optical functions of a thin film

The first example demonstrates how IMD can be used to visualize multidimensional optical functions: We present the results of a computation of the reflectance and transmittance of an amorphous carbon film[15] on an amorphous SiO_2 substrate, determined as a function of three independent variables: wavelength, for 150 nm $< \lambda < 2.0$ μm, i.e., from the ultraviolet (UV) to the infrared; incidence angle, for $0° < \theta < 90°$; and film thickness, for 0 Å $< d < 1000$ Å.

To visualize the results of this computation, one might imagine displaying one-dimensional graphs of R and T, for example, as a continuous function of one variable, θ, say, and for discrete values of λ and d. Or, perhaps it would be more useful to display a plot in two dimensions, as a continuous function of two variables, and for discrete values of the remaining independent variable. The IMDXPLOT widget, which is the interactive visualization tool in IMD, indeed allows the user to display such ''slices'' of the optical functions, in either one or two dimensions. For example,
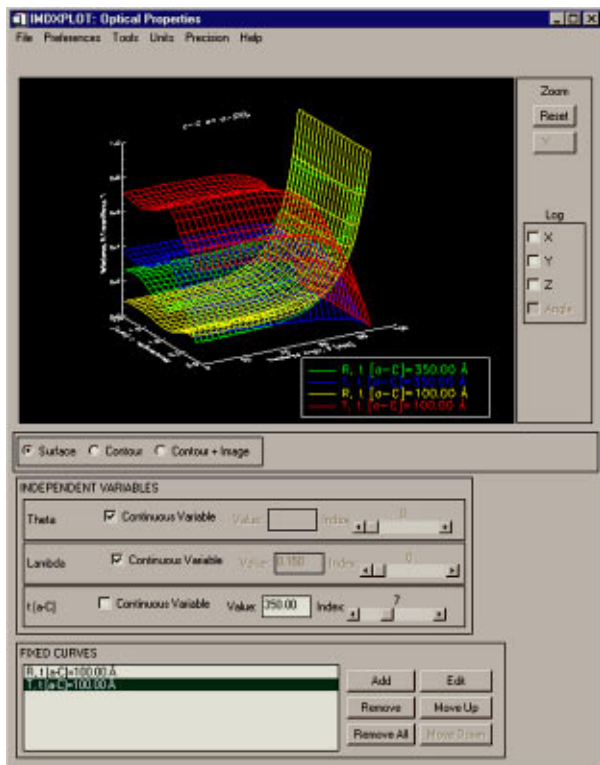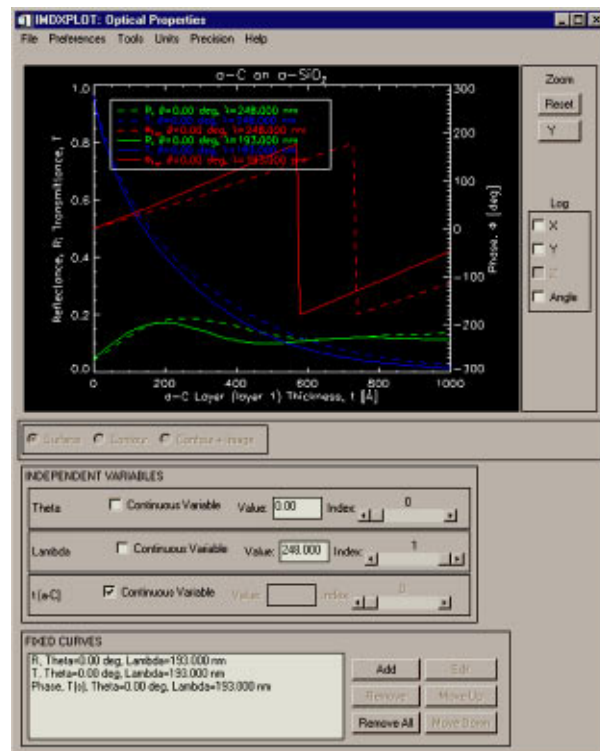

Figure 7. (a) The IMD parameter estimation and confidence interval widget (configured for the curve-fitting example in Sec. III C) and (b) a typical fit parameter widget (configured for the confidence interval computation example in Sec. III D).

presented in Fig. 8 are some of the results of the computation just described. Figure 8(a) shows superposed two-dimensional surface plots of $R(\theta, \lambda)$ and $T(\theta, \lambda)$, for two discrete values of the film thickness, 100 and 350 Å. In Fig. 8(b), on the other hand, are one-dimensional plots of $R(d)$ and $T(d)$, as well as the transmitted phase, $\phi_T(d)$, at normal incidence, for two discrete wavelengths, 193 and 248 nm (i.e., the wavelengths used for DUV lithography). Using the buttons, sliders, and menu options available on the IMDXPLOT interface, the user can easily display such slices through parameter space and customize the graphs according to his/her preference: multiple optical functions can be superposed, the appearance (i.e., colors, line styles, plotting symbols, etc.) of the different functions can be adjusted, and various legends and plot labels can be generated. Additionally, the sliders associated with each of the independent variables (shown in the INDEPENDENT VARIABLES region of the IMDXPLOT widgets in Fig. 8, for example) can be used to vary in real time one or more independent variables and view the resulting effect on the optical functions. A variety of standard graphics file formats (i.e., PostScript, PCL, HPGL, and CGM) is available for output.

(a)

(b)

Figure 8. Results of the computation of reflectance and transmittance of an amorphous carbon film on an amorphous SiO_2 substrate, described in the text. (a) The IMDXPLOT widget showing two-dimensional surface plots of reflectance and transmittance versus incidence angle and wavelength for discrete values of the carbon film thickness. (b) One-dimensional plots of reflectance, transmittance, and transmitted phase versus film thickness, at normal incidence, and for two discrete wavelengths.

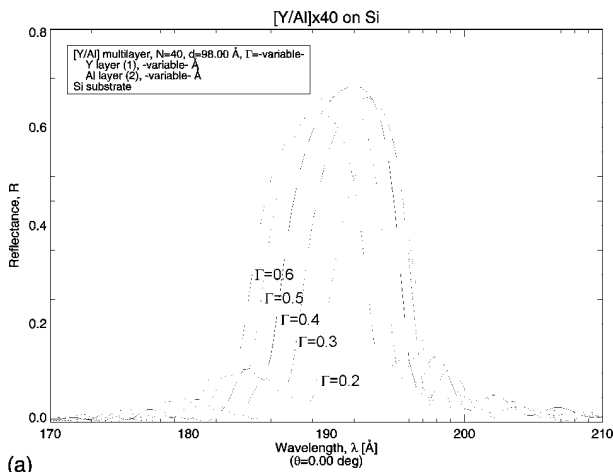## B. Reflectance and electric field intensity for an x-ray multilayer film

The second example shows how IMD can be used to adjust, for optimal performance, design-parameter values of a periodic multilayer. A determination of the electric-field intensity in a periodic multilayer film is presented as well. Shown in Fig. 9(a) is an IMD-generated plot showing the normal incidence soft x-ray reflectance of a Y/Al periodic multilayer film ($d = 90$ Å, $N = 40$) as a function of one particular design parameter, the film-thickness ratio, Γ (where $\Gamma \equiv d_Y / (d_Y + d_{Al})$). By using IMD to compute $R(\Gamma)$, the optimal value of Γ (i.e., giving the highest peak reflectance) is immediately evident. Optimized values of other design parameters can be similarly obtained.

Displayed in Fig. 9(b) is an IMDXPLOT widget showing the electric-field intensity as a function of depth for the $\Gamma = 0.5$ Y/Al multilayer for two values of λ. Observation of the position of the local maxima of the electric-field intensity in the standing-wave pattern at $\lambda = 192$ Å (i.e., the wavelength corresponding to the peak reflectance) suggests, for example, that any interface imperfections at the Al-on-Y interfaces, where the electric-field intensity is strongest, might have a much different effect on the peak reflectance than interface imperfections at the Y-on-Al interfaces, where the electric-field intensity is much weaker.
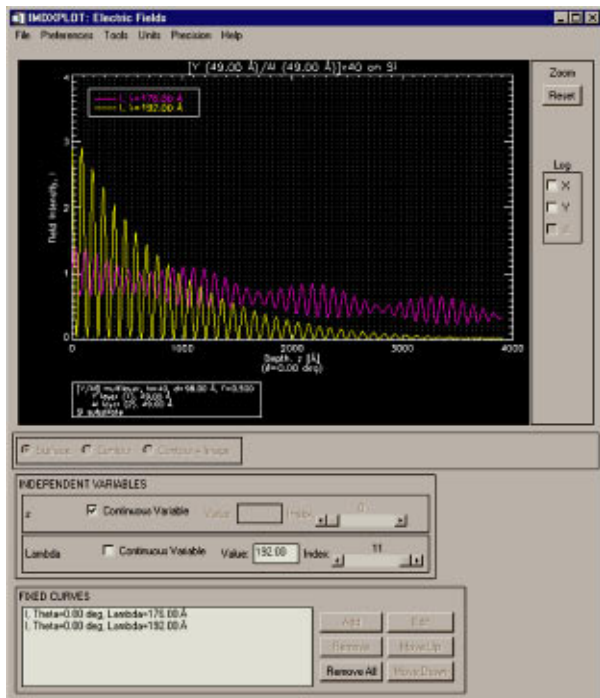
C. XRR analysis of a W/Cr bilayer

The third example demonstrates how the unique ability in IMD to interactively vary model parameters ''manually'' can be used in conjunction with the nonlinear, least-squares fitting capability to accurately determine a large number of film parameters from experimental data.

Shown in Fig. 10 are the measured and calculated curves of grazing-incidence x-ray reflectance versus incidence angle for a W/Cr-bilayer thin film. These particular films are currently being used as the electron-scattering layers in masks for a projection electron-beam-lithography tool (SCALPEL®), currently being developed,[16] in which the image contrast achieved at the focal plane of the tool depends critically on the W- and Cr-layer thicknesses and densities. A precise measurement of these parameters is thus required, and such a measurement can be obtained through the use of XRR analysis, using the curve-fitting techniques described in Sec. I B. However, even for these relatively simple bilayer films, there are additional parameters in the model that must be varied in order to fit the data with sufficient accuracy. For example, the best-fit curve shown in Fig. 10 (labeled $\sigma = 3.5$ Å) was obtained by fitting eight adjustable parameters: the densities, layer thicknesses, and interface roughnesses of both the W and Cr layers, as

Figure 10. *Measured grazing incidence x-ray reflectance for a W/Cr-bilayer film (filled circles) and calculated reflectance curves for different values of the W-layer interfacial roughness (as indicated).*

(b)

Figure 9. *(a) Reflectance of a Y/Al periodic multilayer film as a function of the film-thickness ratio,* Γ. *(b) Electric-field intensity as a function of depth into the film for two wavelengths.*

well as the thickness and roughness of a top-layer oxide (WO$_3$) that forms on these films.

In order to utilize nonlinear, least-squares curve fitting to determine fit parameters, the choice of initial parameter values must be relatively close to the final, best-fit values, or else the fitting algorithm will be unable to locate the global minimum in parameter space corresponding to the minimum value of the χ^2 statistic. This point is especially true in this particular example, where the fitting was performed with so many adjustable parameters. The ability in IMD to first vary parameters manually (as described in Sec. III B) and to visualize in real time the resulting effect on the optical functions (reflectance, in this case), greatly fa-
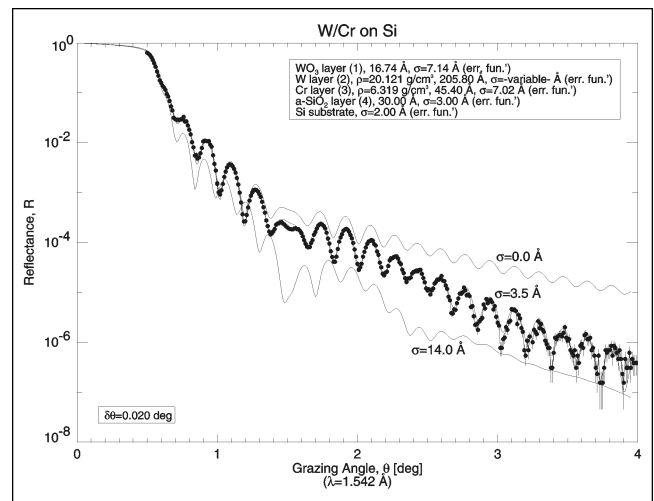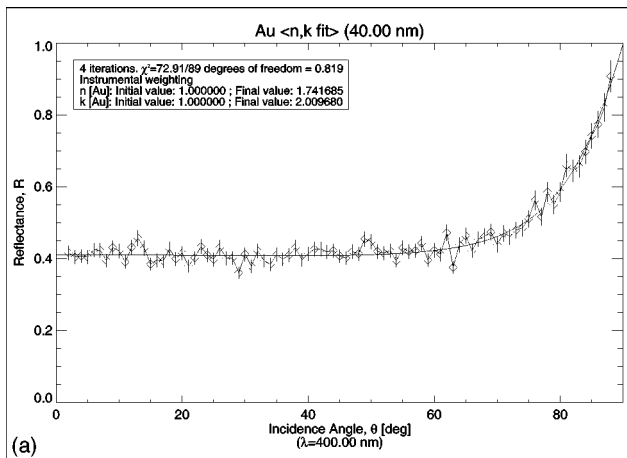
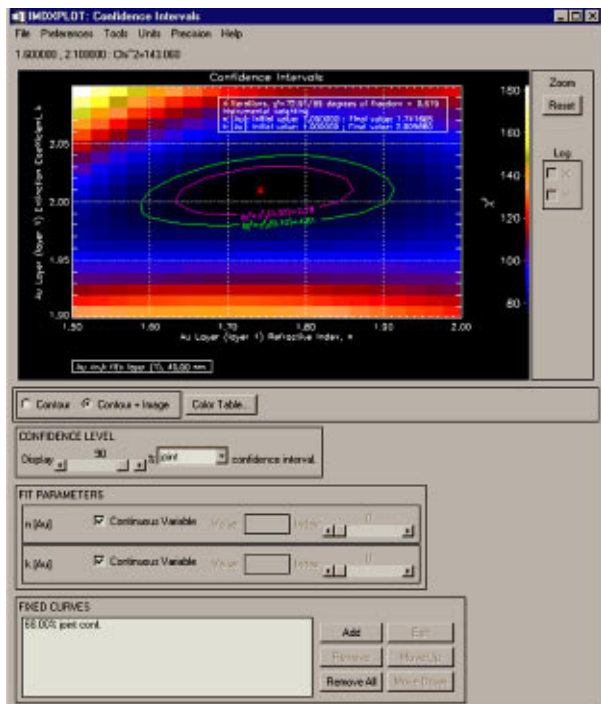cilitates the task of determining initial fit-parameter values.

To illustrate, in order to fit the data shown in Fig. 10, one might start (using bulk densities) by manually varying the W- and Cr-layer thicknesses, until both the high-frequency and low-frequency modulations in the calculated reflectance are reasonably coincident with those in the measured data. These two superposed modulations (seen in Fig. 10 as having periods of ~0.18° and ~1.0°) correspond to interference due to the total film thickness (i.e., WO$_3$+W +Cr layer thicknesses) and the Cr layer thickness, respectively. Therefore, it is especially useful to be able to manually vary two (or more) layer thicknesses in a single calculation and to view the results interactively using IMDXPLOT in order to match both modulations simultaneously. Nonetheless, the W- and Cr-layer thicknesses will generally need significant refinement once other parameters are varied as well, since the effect on the reflectance of other adjustable parameters is effectively coupled to the layer thicknesses. An example of such a coupling can be seen in Fig. 10, where reflectance curves are shown for several values of the W-layer roughness: it can be seen that the thickness modulations shift significantly with roughness (σ), an effect that cannot be completely decoupled from the effect of the individual layer thicknesses.

D. Optical constants determination for a thin film

The final example illustrates the ability in IMD to compute confidence intervals in order to estimate the precision of fit parameters determined from nonlinear, least-squares curve fitting. Shown in Fig. 11(a) are the results of nonlinear, least-squares curve fitting to determine, from reflectance versus incidence-angle measurements, the optical constants (n and k) for a thin film. Once the best-fit parameters were found [as indicated in Fig. 11(a)], the value of the χ^2 statistic S was computed over a grid of points in parameter space, as was described in Sec. I B2. The results of this computation are displayed in the IMDXPLOT widget

Figure 11. (a) Results of nonlinear, least-squares curve fitting to determine, from reflectance vs incidence-angle measurements, the optical constants (n and k) for a gold film. (b) An IMDXPLOT widget showing joint confidence intervals associated with the best-fit values of the optical constants.

shown in Fig. 11(b), where the contours of constant S are shown in two dimensions, corresponding to the 68% (i.e., 1-σ) and 95% (2-σ) joint confidence regions. The IMDX-PLOT sliders in this case can be used to vary the value of $\Delta S(\alpha')$ [see Eq. (18)], or to vary the parameter values when displaying contours of constant S in one dimension (not shown).

IV. SUMMARY

We have described the physics and algorithms on which the IMD computer program is based and have presented a number of examples that illustrate some of IMD's unique capabilities.

Future enhancements to IMD's capabilities will include the ability to compute nonspecular (diffuse) scattered intensity due to interfacial roughness, the ability to define depth-graded thickness and interface parameters, and tools to allow the user to further analyze interactively the computed optical functions (e.g., minimum and maximum values, feature widths, averages, integrals, etc.). The software is available and free, and can be downloaded from the Web site listed in Ref. 2.

REFERENCES

1. See, for example, *Handbook of Optical Constants of Solids*, edited by E. D. Palik (Academic, New York, 1985).
2. IMD can be downloaded from http://www.bell-labs.com/user/windt/idl.
3. B. L. Henke, E. M. Gullikson, and J. C. Davis, At. Data Nucl. Data Tables **54**, (1993). In addition to the data contained therein, the Center For X-Ray Optics (CXRO), Lawrence Berkeley Laboratory, maintains an active database of atomic scattering factors; these data are available at http://www-cxro.lbl.gov and have been included in IMD, courtesy of E. M. Gullikson.
4. IDL is available from Research System, Inc., Boulder, CO, http://www.rsinc.com.
5. See, for example, J. D. Jackson, *Classical Electrodynamics*, 2nd ed. (Wiley, New York, 1975), pp. 281–282.
6. Note that in our definition of the Fresnel coefficients we have assumed that (a) each material is optically isotropic, and (b) the magnetic permeability is the same in both regions.
7. D. G. Stearns, J. Appl. Phys. **65**, 491 (1989).
8. L. Névot and P. Croce, Rev. Phys. Appl. **15**, 761 (1980).
9. M. Born and E. Wolf, *Principles of Optics*, 6th ed. (Pergamon, Oxford, 1980).
10. D. W. Marquardt, J. Soc. Ind. Appl. Math. **11**, 431 (1963).
11. P. R. Bevington, *Data Reduction and Error Analysis for the Physical Sciences* (McGraw–Hill, New York, 1969).
12. M. Lampton, B. Margon, and S. Bowyer, Astrophys. J. **208**, 177 (1976).
13. W. Cash, Astron. Astrophys. **52**, 307 (1976).
14. A periodic multilayer is defined here as a group of *m* layers that is repeated *N* times to make a stack consisting of a total of $m \times N$ layers.
15. Due to the particular optical properties of amorphous carbon films, namely, the 180° phase change for transmittance values near 10% at certain deep UV wavelengths that are used in photolithography for the manufacture of integrated circuits, phase-shift masks (used to compensate for the effects of diffraction in order to print features smaller than the exposure wavelength) made from such films are currently being developed. Such films are also being developed for use as variable transmission apertures, which can be used to greatly enhance the process latitude of DUV lithography tools. See, for example, R. A. Cirelli, M. Mkrtchyn, G. P. Watson, L. E. Trimble, G. R. Weber, D. L. Windt, and O. Nalamasu, Proc. SPIE **3334**, (1998).
16. See http://www.lucent.com/SCALPEL for a complete bibliography of papers describing SCALPEL technology.